Hindawi Publishing Corporation
Journal of Nanomaterials
Volume 2012, Article ID 486284, 5 pages
doi:10.1155/2012/486284

Research Article

Magnetic and Electric Properties of Amorphous $Co_{40}Fe_{40}B_{20}$ Thin Films

Yuan-Tsung Chen and S. M. Xie

Department of Materials Science and Engineering, I-Shou University, Kaohsiung Taiwan 840, Taiwan

Correspondence should be addressed to Yuan-Tsung Chen, ytchen@isu.edu.tw

Received 23 September 2011; Revised 19 October 2011; Accepted 16 November 2011

Academic Editor: Donglu Shi

$C_{40}Fe_{40}B_{20}$ was deposited on a glass substrate to a thickness (t_f) of between 100 Å and 500 Å. X-ray diffraction patterns (XRD) indicate that $C_{40}Fe_{40}B_{20}$ films are in an amorphous state. The plane-view microstructures and grain size distributions of CoFeB thin films are observed under a high-resolution transmission electron microscope (HRTEM). The thicker CoFeB films have larger grain size distribution than thinner CoFeB films. The saturation magnetization (M_s) exhibits a size effect, meaning that M_s increases as t_f increases. The magnetic remanence magnetization (M_r) of CoFeB thin films are sensitive to thinner CoFeB films, and the refined grain size of thinner CoFeB films can induce ferromagnetic stronger spin exchange-coupling behavior than thicker CoFeB films, resulting in higher remanence. The highest magnetic squareness ratio (M_r/M_s) of the CoFeB films occurs at thickness of 100 Å, suggesting the 100 Å of the as-deposited CoFeB film is suitable for magnetic memory application. These results also demonstrate that coercivity (H_c) is increased by an increase in the width of the distribution of grain sizes. The electrical resistivity (ρ) of such a film is typically higher than normally exceeding 100 $\mu\Omega$ cm, revealing that the amorphous phase dominates. These results are consistent with the XRD results.

1. Introduction

Amorphous structures in materials exhibit exceptional characteristics, including high strength and hardness. They also are associated with superior wear resistance in a bulk metallic glass (BMG) matrix. $Co_{40}Fe_{40}B_{20}$ magnetic thin films have just such an amorphous structure [1–5]. Almost nothing has been reported on corning amorphous magnetic materials. Amorphous $Co_{40}Fe_{40}B_{20}$ free/pinned layer of spin value is expected to be applied in magnetoresistance (MR) read-out heads for density magnetic recording applications. $Co_{40}Fe_{40}B_{20}$ magnetic thin films have attracted increasing attention owing to their use in applications that involve giant magnetoresistance (GMR), tunneling magnetoresistance (TMR), and magnetoresistance random access memory (MRAM), because of their low coercivity (H_c) and high spin polarization. The material is generally inserted into a free, pinned ferromagnetic component because of its spin value [6–10]. The material has a high spin-dependent scattering, lower coercivity, and stronger spin tunneling effect and therefore supports a higher output signal for particular GMR and TMR ratios in amorphous CoFeB/Ru/CoFeB, CoFeB/AlO_x/CoFeB, and CoFeB/MgO/CoFeB magnetic tunnel junctions (MTJs). The very short electron mean free path in amorphous alloys yields a higher magnetoresistance (MR) ratios [11–15]. Since the mean free path is much shorter in amorphous materials than in crystalline materials, the dependence of the MR ratio on thickness is believed to differ markedly between them. Briefly, amorphous $Co_{40}Fe_{40}B_{20}$ thin film exhibits favorable mechanical properties and a high TMR ratio because of its amorphous structure and increased spin polarization.

This investigation elucidated the structure, magnetic properties, and electrical properties of $Co_{40}Fe_{40}B_{20}$ thin films using X-ray diffraction (XRD), a high-resolution transmission electron microscope (HRTEM), a superconducting quantum interference device (SQUID), and a traditional four-point sheet resistance meter, respectively. The XRD diffraction results confirm that CoFeB thin films have an amorphous state. The grain size distribution is employed

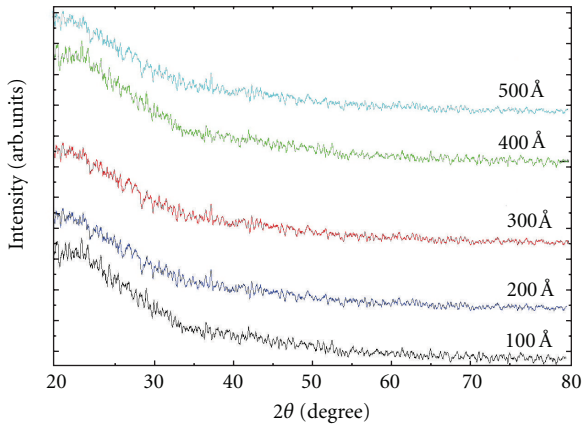

Figure 1: XRD patterns of CoFeB thin films.

by plane-view HRTEM. The electrical resistivity (ρ) and resistance (R) also reveal that the $Co_{40}Fe_{40}B_{20}$ thin film is in an amorphous state. The saturation magnetization (M_s) results indicate a size effect, which increases with the thickness of CoFeB from 100 Å to 500 Å. It means the thinner CoFeB films can enhance ferromagnetic higher spin-exchange coupling effect than thicker CoFeB films. Grain refinement induces ferromagnetic spin-exchange coupling behavior, increasing the magnetic squareness ratio of thinner CoFeB films. Coercivity (H_c) is sensitive to the grain size effect of the films, suggesting that H_c increases with the enlarged grain distribution.

2. Experimental Details

CoFeB thin films were deposited on a glass substrate at room temperature (RT) by dc magnetron sputtering with a thicknesses (t_f) between 100 Å and 500 Å. The typical base chamber pressure exceeded 1.5×10^{-7} Torr, and the Ar working chamber pressure was 2×10^{-3} Torr. The target composition of the CoFeB alloy was 40 at.% Co, 40 at.% Fe, and 20 at.% B.

The structure of the CoFeB thin film was characterized using XRD with a $CuK_{\alpha 1}$ line (Philips X'pert). To determine the grain size distribution and the average grain size, a plane-view microstructure was obtained using high-resolution transmission electron microscope (HRTEM, JEOL-2100F). The in-plane magnetic hysteresis loop of the CoFeB films was obtained using a superconducting quantum interference device (SQUID). To examine the electrical properties of the CoFeB thin films at room temperature, a traditional four-point sheet resistance meter was utilized.

3. Results and Discussion

Figure 1 presents the X-ray diffraction pattern (XRD) of the CoFeB thin films. These results demonstrate that all of the as-deposited CoFeB thin films herein are in an amorphous state, yielding no apparent diffraction peak.

Figures 2(a) to 2(e) present the typical plane-view microstructures and grain size distributions of all CoFeB films from 100 Å to 500 Å, obtained using HRTEM, respectively. From the TEM observation, the result shows that the distribution of very small grain sizes exists at CoFeB thin films. It indicates that the as-deposited microstructure of CoFeB thin films is of amorphous or very fine nanocrystalline state, because the HRTEM resolution is stronger than XRD measurement. The grain sizes of thicker CoFeB thin films are generally thinner than CoFeB thin films.

Figure 3(a) displays the saturation magnetization (M_s) and remanent magnetization (M_r) of CoFeB thin films. The figure reveals that M_s increases linearly with film thickness whereas M_r exponentially decreases. This figure suggests that CoFeB thin films exhibit a size effect, meaning that M_s increases owing to spin ferromagnetic coupling as t_f is increased from 100 Å to 500 Å. In contrast, M_r decreases as t_f is increased from 100 Å to 500 Å. The refinement of grains in thinner CoFeB films reduces the effective anisotropy constant, increases the effective spin exchange range, induces ferromagnetic spin-exchange coupling, and thereby increases the remanent magnetization and the squareness ratio (M_r/M_s) [16]. The magnetic squareness ratio (M_r/M_s) of the as-deposited CoFeB films, an important parameter, is highest at a thickness of 100 Å. The disturbed read/write signals of a magnetic device decrease, suggesting that the as-deposited CoFeB film with a thickness of 100 Å is effective in MRAM. Figure 3(b) plots the relationship between coercivity (H_c) and magnetic spin switch state of amorphous CoFeB thin films. H_c increases with t_f. This result is consistent with the grain size effect [17, 18], indicating that larger grains are associated with higher H_c.

Figure 4 plots the resistance (R) of the CoFeB films. The corresponding electrical resistivity value (ρ) is calculated using the following formula [19], as also displayed in Figure 4. The resistance and electrical resistivity are reduced as the CoFeB thickness increases. The R values range from 150 Ω to 22 Ω, and the ρ values are form 245 $\mu\Omega$ cm to 133 $\mu\Omega$ cm as t_f increases from 100 Å to 500 Å. The electrical resistivity is given by

$$R = \frac{\rho L}{A}. \tag{1}$$

R and ρ are the resistance and electrical resistivity of the material, respectively. L represents the conductive path of the electron. A denotes the cross-sectional area of the material and width is A/t_f. Grain boundaries and the surface of thin films scatter the electrons, and so thinner films have higher resistance than thicker films. The electrical resistivity (ρ) of such a film is generally higher than normal exceeding 100 $\mu\Omega$ cm, revealing that the amorphous phase dominates. These results are consistent with the XRD data.

4. Conclusions

This study investigates the structure, magnetic parameters, and electric properties of amorphous CoFeB thin films. XRD indicates that CoFeB thin films are in an amorphous state and yield no apparent diffraction peak. To observe the grain size distribution, the plane-view HRTEM shows

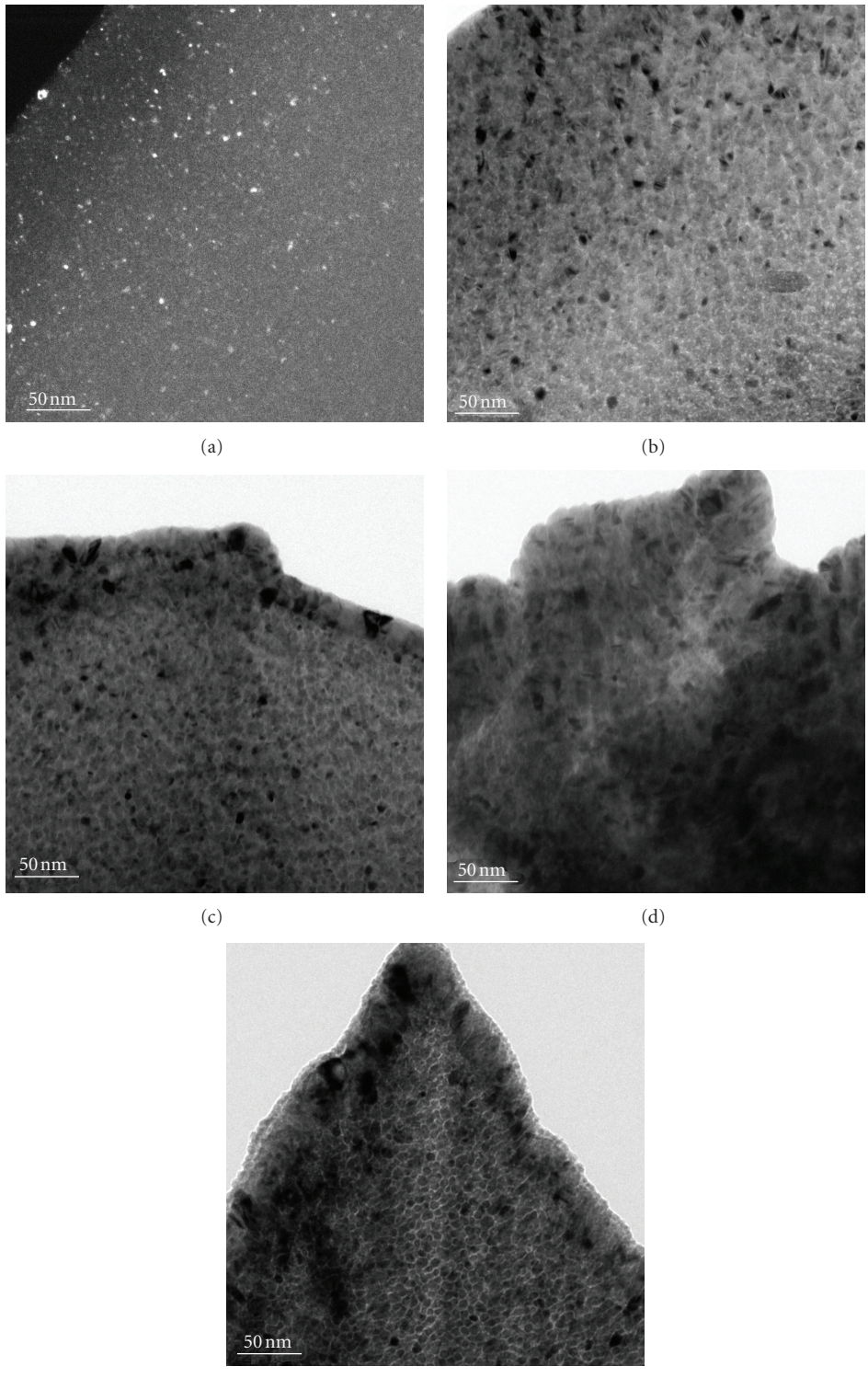

Figure 2: Plane-view HRTEM images of as-deposited CoFeB thin films. (a) 100 Å, (b) 200 Å, (c) 300 Å, (d) 400 Å, and (e) 500 Å.

that the thicker CoFeB thin films are generally larger than thinner CoFeB thin films. The resistance (R) and electrical resistivity (ρ) of CoFeB thin films are consistent with the XRD results. Results concerning the magnetic properties demonstrate that the saturation magnetization (M_s) of CoFeB films is affected by size and that refinement of grains improves ferromagnetic spin exchange coupling, increasing the remanent magnetization (M_s) and squareness ratio. The important parameter of highest magnetic squareness ratio (M_r/M_s) of the as-deposited CoFeB films occurs at

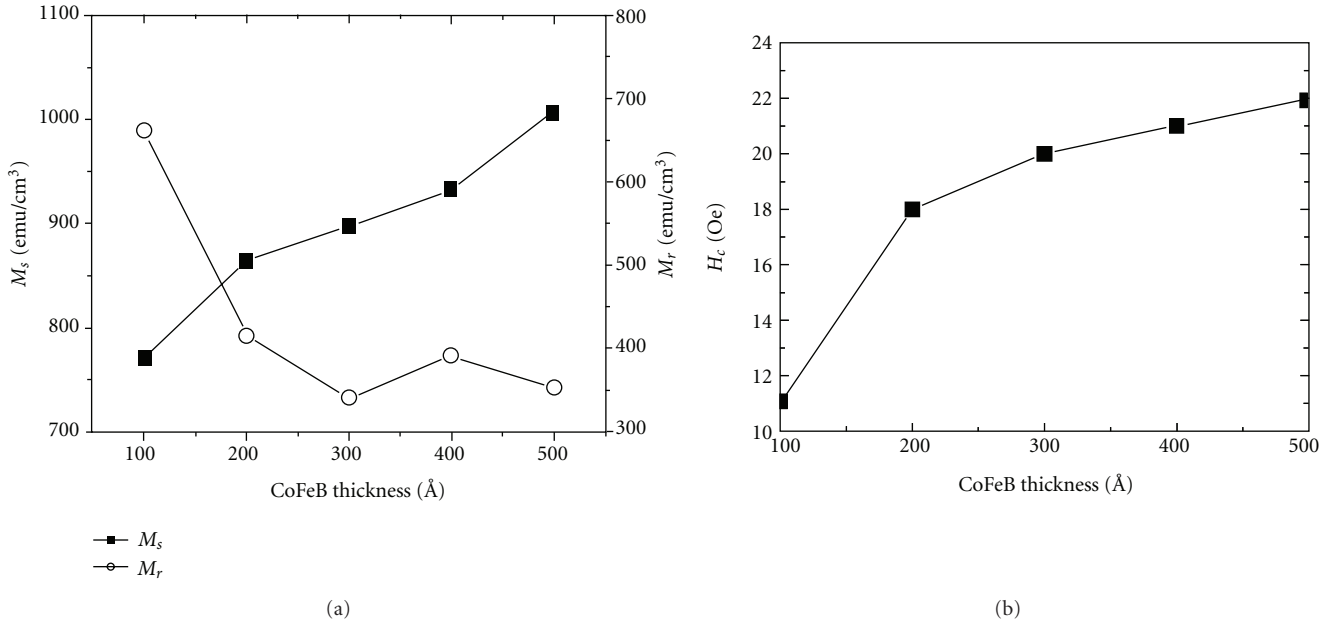

Figure 3: Saturation magnetization (M_s), remanent magnetization (M_r), and coercivity (H_c) of amorphous CoFeB films. (a) Saturation magnetization (M_s) and remanent magnetization (M_r) and (b) coercivity (H_c).

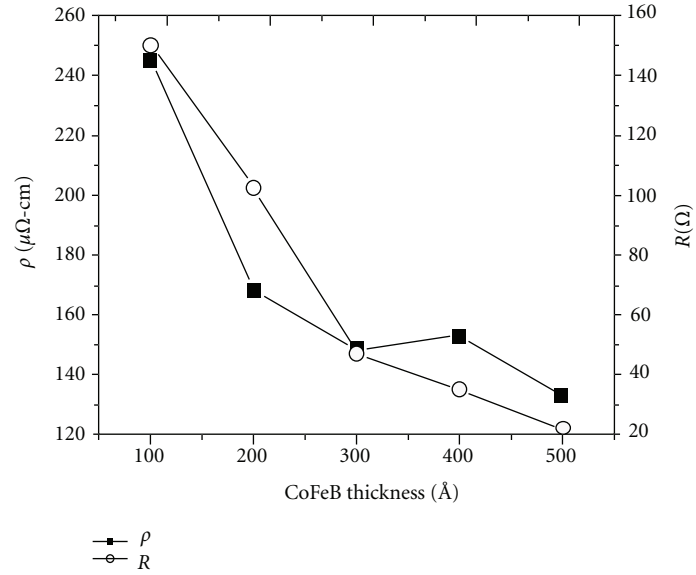

Figure 4: Resistance (R) and electrical resistivity values (ρ) as a function of CoFeB thickness.

thickness of 100 Å, suggesting the thickness of 100 Å of the as-deposited CoFeB film is suitable for magnetic memory application. Finally, the coercivity (H_c) is also associated with the distribution of the grain sizes.

Acknowledgments

This work was supported by the National Science Council, under Grant no. NSC100-2112-M-214-001-MY3.

References

[1] J. S. C. Jang, C. F. Chang, Y. C. Huang, J. C. Huang, W. J. Chiang, and C. T. Liu, "Viscous flow and microforming of a Zr-base bulk metallic glass," *Intermetallics*, vol. 17, no. 4, pp. 200–204, 2009.

[2] C. J. Gilbert, J. M. Lippmann, and R. O. Ritchie, "Fatigue of a Zr-Ti-Cu-Ni-Be bulk amorphous metal: stress/life and crack-growth behavior," *Scripta Materialia*, vol. 38, no. 4, pp. 537–542, 1998.

[3] A. Inoue, B. Shen, H. Koshiba, H. Kato, and A. R. Yavari, "Cobalt-based bulk glassy alloy with ultrahigh strength and

soft magnetic properties," *Nature Materials*, vol. 2, no. 10, pp. 661–663, 2003.

[4] W. L. Johnson, "Bulk glass-forming metallic alloys: science and technology," *MRS Bulletin*, vol. 24, no. 10, pp. 42–56, 1999.

[5] J. S. C. Jang, S. R. Jian, D. J. Pan, Y. H. Wu, J. C. Huang, and T. G. Nieh, "Thermal and mechanical characterizations of a Zr-based bulk metallic glass composite toughened by in-situ precipitated Ta-rich particles," *Intermetallics*, vol. 18, no. 4, pp. 560–564, 2010.

[6] C. Y. You, H. S. Goripati, T. Furubayashi, Y. K. Takahashi, and K. Hono, "Exchange bias of spin valve structure with a top-pinned $Co_{40}Fe_{40}B_{20}$ IrMn," *Applied Physics Letters*, vol. 93, no. 1, Article ID 012501, 3 pages, 2008.

[7] J. Hayakawa, S. Ikeda, Y. M. Lee et al., "Current-driven magnetization switching in CoFeB/MgO/CoFeB magnetic tunnel junctions," *Japanese Journal of Applied Physics, Part 2*, vol. 44, no. 37–41, pp. L1267–L1270, 2005.

[8] Y. M. Lee, J. Hayakawa, S. Ikeda, F. Matsukura, and H. Ohno, "Giant tunnel magnetoresistance and high annealing stability in CoFeB/MgO/CoFeB magnetic tunnel junctions with synthetic pinned layer," *Applied Physics Letters*, vol. 89, no. 4, Article ID 042506, 3 pages, 2006.

[9] C. Y. You, T. Ohkubo, Y. K. Takahashi, and K. Hono, "Boron segregation in crystallized MgO/amorphous- $Co_{40}Fe_{40}B_{20}$ thin films," *Journal of Applied Physics*, vol. 104, no. 3, Article ID 033517, 6 pages, 2008.

[10] T. Aoki, Y. Ando, D. Watanabe, M. Oogane, and T. Miyazaki, "Spin transfer switching in the nanosecond regime for CoFeB/MgO/CoFeB ferromagnetic tunnel junctions," *Journal of Applied Physics*, vol. 103, no. 10, Article ID 103911, 4 pages, 2008.

[11] D. H. Lee and S. H. Lim, "Increase of temperature due to Joule heating during current-induced magnetization switching of an MgO-based magnetic tunnel junction," *Applied Physics Letters*, vol. 92, no. 23, Article ID 233502, 3 pages, 2008.

[12] H. X. Wei, Q. H. Qin, M. Ma, R. Sharif, and X. F. Han, "80% tunneling magnetoresistance at room temperature for thin Al-O barrier magnetic tunnel junction with CoFeB as free and reference layers," *Journal of Applied Physics*, vol. 101, no. 9, Article ID 09B501, 3 pages, 2007.

[13] S. K. Wang, Y.-T. Chen, and S. R. Jian, "Determining contact angle and surface energy of $C_{60}Fe_{60}B_{20}$ thin films by magnetron sputtering," *Journal of Nanomaterials*, vol. 2011, Article ID 291935, 4 pages, 2011.

[14] T. Aoki, Y. Ando, M. Oogane, and H. Naganuma, "Reproducible trajectory on subnanosecond spin-torque magnetization switching under a zero-bias field for MgO-based ferromagnetic tunnel junctions," *Applied Physics Letters*, vol. 96, no. 14, Article ID 142502, 3 pages, 2010.

[15] S. Isogami, M. Tsunoda, K. Komagaki et al., "In situ heat treatment of ultrathin MgO layer for giant magnetoresistance ratio with low resistance area product in CoFeB/MgO/CoFeB magnetic tunnel junctions," *Applied Physics Letters*, vol. 93, no. 19, Article ID 192109, 3 pages, 2008.

[16] Z. Q. Jin, N. N. Thadhani, M. McGill et al., "Grain size dependence of magnetic properties in shock synthesized bulk $Pr_2Fe_{14}B/\alpha$-Fe nanocomposites," *Journal of Applied Physics*, vol. 96, no. 6, pp. 3452–3457, 2004.

[17] M. Yoshino, Y. Kikuchi, A. Sugiyama, and T. Osaka, "Preparation of high magnetic flux density CoNiFeB film by electroless deposition for application to magnetic recording devices," *Electrochimica Acta*, vol. 53, no. 2, pp. 285–289, 2007.

[18] W. S. Sun, T. Kulik, X. B. Liang, and J. Ferenc, "Thermal stability and magnetic properties of Co-Fe-Hf-Ti-Mo-B bulk metallic glass," *Intermetallics*, vol. 14, no. 8-9, pp. 1066–1068, 2006.

[19] Y. Han, C. Gao, Y. Ma et al., "Integrated microcircuit on a diamond anvil for high-pressure electrical resistivity measurement," *Applied Physics Letters*, vol. 86, no. 6, Article ID 064104, 3 pages, 2005.